Letter

Coupled frustrated ferromagnetic and antiferromagnetic quantum spin chains in the quasi-one-dimensional mineral antlerite $Cu_3SO_4(OH)_4$

Anton A. Kulbakov,[1] Denys Y. Kononenko,[2] Satoshi Nishimoto,[2,3] Quirin Stahl,[1] Aswathi Mannathanath Chakkingal,[1] Manuel Feig,[4] Roman Gumeniuk,[4] Yurii Skourski,[5] Lakshmi Bhaskaran,[5] Sergei A. Zvyagin,[5] Jan Peter Embs,[6] Inés Puente-Orench,[7,8] Andrew Wildes,[8] Jochen Geck,[1,9] Oleg Janson,[2,*] Dmytro S. Inosov,[1,9,†] and Darren C. Peets[1,‡]

[1]*Institut für Festkörper- und Materialphysik, Technische Universität Dresden, 01069 Dresden, Germany*
[2]*Leibniz Institute for Solid State and Materials Research Dresden, 01069 Dresden, Germany*
[3]*Institut für Theoretische Physik, Technische Universität Dresden, 01069 Dresden, Germany*
[4]*Institut für Experimentelle Physik, TU Bergakademie Freiberg, 09596 Freiberg, Germany*
[5]*Dresden High Magnetic Field Laboratory (HLD-EMFL), Helmholtz-Zentrum Dresden-Rossendorf, 01328 Dresden, Germany*
[6]*Laboratory for Neutron Scattering and Imaging, Paul Scherrer Institut, 5232 Villigen, Switzerland*
[7]*Instituto de Nanociencia y Materiales de Aragón (INMA), CSIC-Universidad de Zaragoza, Zaragoza 50009, Spain*
[8]*Institut Laue-Langevin, 71 Avenue des Martyrs, CS 20156, CEDEX 9, 38042 Grenoble, France*
[9]*Würzburg-Dresden Cluster of Excellence on Complexity and Topology in Quantum Matter–ct.qmat, Technische Universität Dresden, 01069 Dresden, Germany*

(Received 28 March 2022; revised 6 July 2022; accepted 11 July 2022; published 28 July 2022)

Magnetic frustration, the competition among exchange interactions, often leads to novel magnetic ground states with unique physical properties which can hinge on details of interactions that are otherwise difficult to observe. Such states are particularly interesting when it is possible to tune the balance among the interactions to access multiple types of magnetic order. We present antlerite $Cu_3SO_4(OH)_4$ as a potential platform for tuning frustration. Contrary to previous reports, the low-temperature magnetic state of its three-leg zigzag ladders is a quasi-one-dimensional analog of the magnetic state recently proposed to exhibit spinon-magnon mixing in botallackite. Density functional theory calculations indicate that antlerite's magnetic ground state is exquisitely sensitive to fine details of the atomic positions, with each chain independently on the cusp of a phase transition, indicating an excellent potential for tunability.

DOI: 10.1103/PhysRevB.106.L020405

Magnetic frustration, wherein the exchange energy cannot be simultaneously minimized on all individual bonds in the spin system, leads to a wide array of novel magnetic phases [1–3]. The ground state can be selected by a delicate balance of interactions, while the cancellation of stronger interactions can bring weaker interactions to the fore, allowing the observation of effects that would ordinarily be hidden or negligible [4]. Magnetic frustration can be achieved either geometrically, where spins populate a lattice whose spatial arrangement forces the interactions to compete, or through longer-range interactions which compete with shorter-range interactions [5–7]. A reduction in dimensionality can also assist in destabilizing conventional magnetic order, by reducing the number of exchange pathways that lower its energy. The richest physics is expected where the energy scales of the interactions and the competition among them either prevent the system from finding a unique ground state, or make multiple spin configurations nearly degenerate, such that the material may be readily tuned among several exotic states. This can be particularly interesting in quantum spin systems, materials with effective spin-$\frac{1}{2}$ moments, where quantum fluctuations also play a significant role.

Divalent Cu materials offer a particularly attractive playground for frustration, since a strong tendency toward Jahn-Teller distortions breaks orbital degeneracy, leading to a half-filled band, in which strong on-site interactions drive localization and favor $S=\frac{1}{2}$ antiferromagnetism. A wide variety of Cu sublattices are realized in natural minerals, predominantly composed of distorted Cu triangular motifs [8], offering a rich playground for frustrated quantum spin physics. As two very recent examples, the coexistence of triplons, spinons, and magnons was reported in $SeCuO_3$ [9], and the interaction of spinons and magnons was reported for the first time in botallackite, $Cu_2(OH)_3Br$ [10]. In the latter, a distorted-triangular Cu plane can be understood as alternating ferro- and antiferromagnetic (AFM) one-dimensional (1D) chains with weaker interchain interactions. The magnetic ground state in botallackite, shown in Fig. 1(e), has now been explained through a combination of first-principles calculations based on density functional theory (DFT), linear spin-wave theory, and exact diagonalization [12], and related systems are now being explored theoretically as the spin model is generalized [13].

*o.janson@ifw-dresden.de
†dmytro.inosov@tu-dresden.de
‡darren.peets@tu-dresden.de

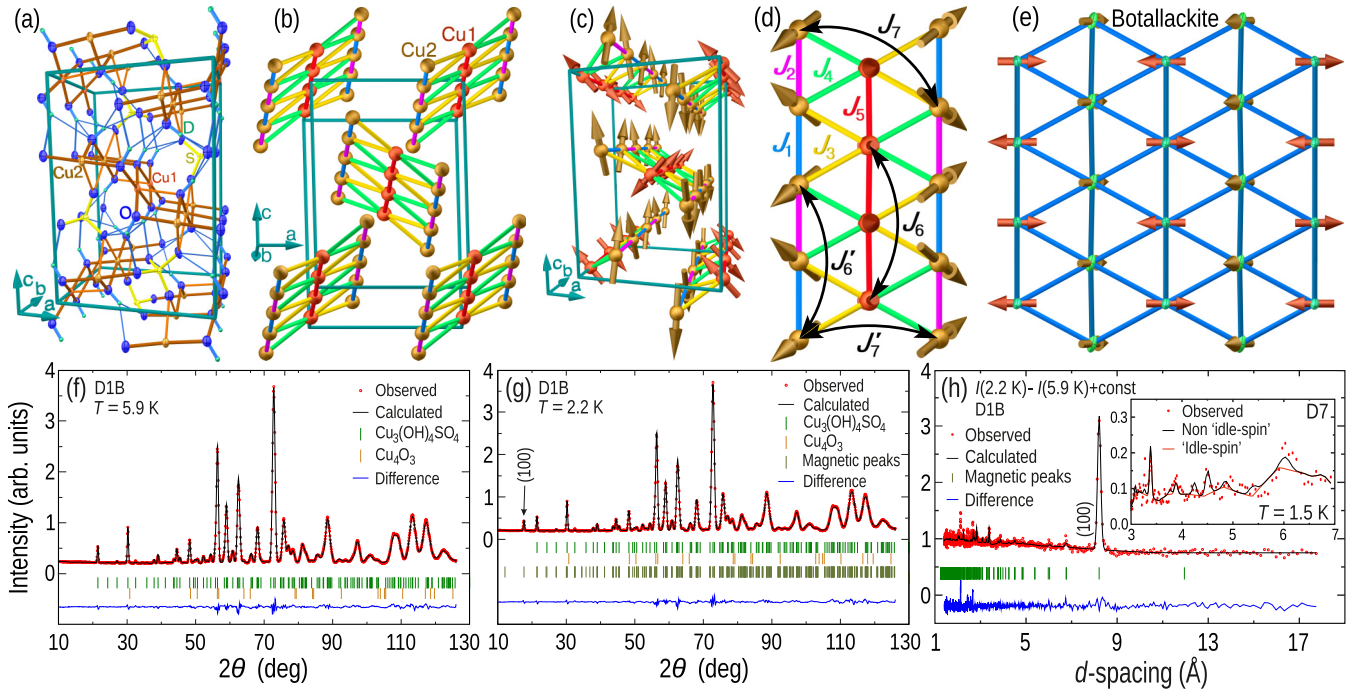

FIG. 1. (a) Crystal structure of $Cu_3SO_4(OD)_4$ from single-crystal x-ray diffraction at 30 K, and 5.9 K neutron powder diffraction. (b) Cu sublattice viewed along the *b* axis. (c) Refined magnetic ground state of antlerite. (d) Exchange interactions within a ladder. (e) Cu sublattice [11] and spin orientations [10] in botallackite for comparison. Neutron powder refinements are shown for (f) the paramagnetic state at 5.9 K and (g) the low-temperature state at 2.2 K. (h) The difference between these datasets. Inset: refinement of spin-polarized neutron diffraction data (D7) with the idle-spin and non-idle-spin magnetic models.

The natural mineral antlerite $Cu_3SO_4(OH)_4$ is a three-leg ladder compound in which zigzag bonds between the central and side legs form triangles of Cu^{2+} ions [14]—its copper sublattice is depicted in Fig. 1(b). Such triangular-lattice ladders have been studied far less than their square-lattice analogs [15], despite the opportunity for strong frustration. Previous neutron diffraction studies on antlerite indicated that only the outer legs of the ladder possess an ordered moment while the central leg exhibits unexplained "idle-spin" behavior [16,17]. However, follow-up studies have seriously questioned this result. DFT calculations showed strong AFM coupling along the central leg of the ladder, which would be expected to induce order [18]. Then, comprehensive specific-heat and proton-NMR measurements in magnetic field [19] found a more complex magnetic phase diagram than previously reported [17], including a phase which can only be realized if the system has at least four distinct magnetic sites. The correct low-temperature magnetic ground state has remained elusive.

In this Letter, we determine the low-temperature magnetic ground state of antlerite and model its magnetic interactions using DFT. It is not idle spin as previously proposed [16]. In a ground state strongly reminiscent of botallackite, the ferromagnetic (FM) outer legs of the ladder are antialigned but noncollinear, while the central leg is AFM with a very different spin orientation. DFT finds that both inner and outer chains are on the cusp of phase transitions. This proximity to multiple quantum phase transitions, and the complex phase diagrams already reported [17,19], suggest a unique ability to tune a state of coupled FM and AFM chains. We anticipate that antlerite could serve as a versatile platform for investigating spinon-magnon interactions and the competition among magnetic ground states.

Antlerite was synthesized hydrothermally under autogenous pressure at 180 °C in a Teflon-lined stainless steel autoclave, from $CuSO_4 \cdot 5H_2O$ (Alfa Aesar, 99%) and $Cu(OH)_2$ (Alfa Aesar, 94%) in distilled or deuterated (Acros Organics, 99.8%D) water. Single-crystal x-ray diffraction data were collected from 30 to 295 K on a Bruker-AXS KAPPA APEX II CCD diffractometer with graphite-monochromated Mo $K\alpha$ radiation using an Oxford Cryosystems N-HeliX cryostat to verify the space group symmetry and atomic positions. Weighted full-matrix least-squares refinements on F^2 were performed with SHELX [20,21] as implemented in WINGX 2014.1 [22]. To determine accurate hydrogen positions and the magnetic structure, high-resolution neutron powder diffraction was performed at D1B [23] and neutron diffraction with polarization analysis using D7 [24], both at the Institut Laue-Langevin, Grenoble, France. Powder diffraction data were Rietveld refined in FULLPROF by the full-matrix least-squares method [25], using the scattering factors from Ref. [26]. The atomic positions, shown in Fig. 1(a) and detailed in the Supplemental Material [27], largely agree with the previously reported structure [14,16], hydrogen positions excepted. The latter are now better aligned with their host oxygen atoms along *c*.

Powder inelastic neutron scattering (INS) was measured on the FOCUS spectrometer at the Paul Scherrer Institute, Villigen, Switzerland [28], using wavelengths of 5 and 6 Å, having energy resolution of 91 and 43 μeV at the elastic line, respectively, and was modeled using SPINW [29]. High-field magnetization of a powder sample was measured at the

Dresden High Magnetic Field Laboratory (HLD), Helmholtz-Zentrum Dresden-Rossendorf (HZDR), Germany, using a 60-T pulsed field magnet with a rise time of 7 ms and a total pulse duration of 25 ms. The magnetization was obtained by integrating the voltage induced in a compensated coil system surrounding the sample [30].

Neutron diffractograms in the paramagnetic state at 5.9 K and in the low-temperature state at 2.2 K are shown in Figs. 1(f) and 1(g), respectively. Additional magnetic intensity on structural Bragg peaks and new weak magnetic peaks were observed at low temperature, as seen in the difference spectrum in Fig. 1(h)—the strongest magnetic reflection, the structurally forbidden (100), is highlighted. Our refinements of the low-temperature ground state do not support the idle-spin model proposed previously [16,17,31], which fails to predict several observed magnetic peaks as shown in the inset to Fig. 1(h). The data are instead best described by a model with propagation vector (100) having AFM order along the central (Cu1) leg of the ladder and significant canting of the other spins, as depicted in Fig. 1(c). The ordered moments on the Cu1 site are $0.80(22)\mu_B$ along $[\pm 0.54(17), 0, \pm 0.59(14)]$, while the ordered Cu2 moments of $0.97(5)\mu_B$ lie along $[0, \pm 0.38(5), \pm 0.89(9)]$ and are ferromagnetically aligned along each side leg. As found previously, the side legs are mutually antialigned. Accounting for g factors of 2.1–2.3 from electron spin resonance (ESR) [27,32] and magnetization [17], this indicates that Cu2 is nearly fully ordered, while a reduced Cu1 moment may arise from the quantum fluctuations expected for $S = \frac{1}{2}$, from frustration, or from the low number of interactions present in this low-dimensional material. Our refined ground state resembles the "AF6" state calculated in Ref. [18] but with significant additional canting.

To determine the isotropic magnetic exchange interactions in antlerite, we performed DFT band-structure calculations using the full-potential local-orbital code FPLO v.18 [33]. We employed a scalar-relativistic treatment within the generalized gradient approximation (GGA) for the exchange and correlation potential [34]. For the structural input, we used our newly refined low-temperature unit cell parameters and atomic coordinates, which are described alongside further details of our calculations in the Supplemental Material [27].

In a nonmagnetic GGA calculation, antlerite features a spurious metallic ground state due to the underestimation of Coulomb repulsion among the Cu $3d$ electrons. An eight-band manifold crossing the Fermi level is due to the antibonding combination of Cu $3d_{x^2-y^2}$ and O $2p_\sigma$ states. We mapped these states onto an effective one-orbital model which is parametrized by projecting the respective GGA bands onto a Wannier basis of Cu $3d_{x^2-y^2}$ states. The parameters of the effective one-orbital model are hopping integrals t_{ij} that describe virtual electron transfer between Cu sites i and j. Nine t_{ij} terms exceeding the threshold of 15 meV are provided in Table I, where we adopt the notation from Refs. [16–18]. In agreement with the previous works, we find that antlerite is a quasi-1D magnet, with sizable hopping interactions confined to the three-leg ladders [35].

To estimate the respective exchange integrals, we doubled the unit cell in the $\boldsymbol{b}$ direction and constructed 64 inequivalent magnetic configurations, whose total energies were calculated on a $2 \times 2 \times 2$ k mesh within the GGA+U approximation.

TABLE I. Leading hopping (t_{ij}, in meV) and exchange (J_{ij}, in K) integrals in antlerite based on our refined structure. Positive exchanges are AFM. The respective intersite distances $d_{\text{Cu-Cu}}$ are given in Å.

Label	$d_{\text{Cu-Cu}}$	t_{ij}	J_{ij}	Type of exchange
J_1	2.980	93	−26	First-neighbor in outer legs
J_2	3.053	73	−11	
J_3	3.240	101	9	Couple central and outer legs
J_4	3.151	103	11	
J_5	3.018	167	48	First-neighbor in central leg
J_6	6.034	56	25	Second-neighbor in central leg
J_6'	6.034	18	6	Second-neighbor in outer legs
J_7	6.391	26	1	Couple outer legs
J_7'	5.634	30	≃0	

To describe interaction effects in the $3d$ shell of Cu, we used the on-site Coulomb repulsion $U = 8.5$ eV, the on-site Hund exchange $J = 1$ eV, and the fully localized limit for the double-counting correction. The resulting total energies are mapped onto a classical Heisenberg model, whose model parameters—the magnetic exchange integrals J_{ij} in Table I—are evaluated by a least-squares solution [27].

While both the crystal and electronic structure of antlerite are shaped by ladders, the backbone of its spin model is the legs, which are coupled by relatively weak J_3 and J_4 exchanges. The central leg hosts competing AFM exchanges J_5 and J_6 operating, respectively, between first and second neighbors. In contrast, the side legs feature alternating first-neighbor FM exchanges J_1 and J_2 and a weaker AFM exchange J_6' between second neighbors the relevance of which, to the best of our knowledge, has not been discussed previously. Finally, while two relevant hoppings connect the side legs, only J_7 gives rise to a small AFM exchange. Our microscopic magnetic model is fundamentally different from the phenomenological model of Ref. [16] and qualitatively similar to the band-structure-based model of Ref. [18]. Despite this qualitative similarity, the ratios such as J_6/J_5 and J_3/J_5, as well as the absolute values of the exchanges, differ significantly, possibly because of the different choice of U, different code, or a high sensitivity of antlerite to perturbations.

We start the discussion of the low-temperature magnetic ground state by considering a simplified spin model of decoupled legs ($J_3 = J_4 = 0$). Here, the central leg would have a helical ground state in the classical model and a gapped phase in the quantum $S = \frac{1}{2}$ case. The side legs would form helices, but in the vicinity of the fully polarized (ferromagnetic) phase; both states are quasiclassical with minor quantum corrections.

When we reinstate the interleg exchanges J_3, J_4, and J_7, the consequent leverage has a drastic impact on the magnetism. At the classical level, a noncollinear state with the central leg twisted into a helix and fully polarized side legs has slightly lower energy than the collinear state which corresponds to the experimental (100) propagation vector. This disagreement may arise from inaccuracies in the exchange integrals, as a collinear state adiabatically connected to the (noncollinear) experimental ground state is found only ∼1.5 K higher in energy than the helical state, well within the uncertainty of DFT.

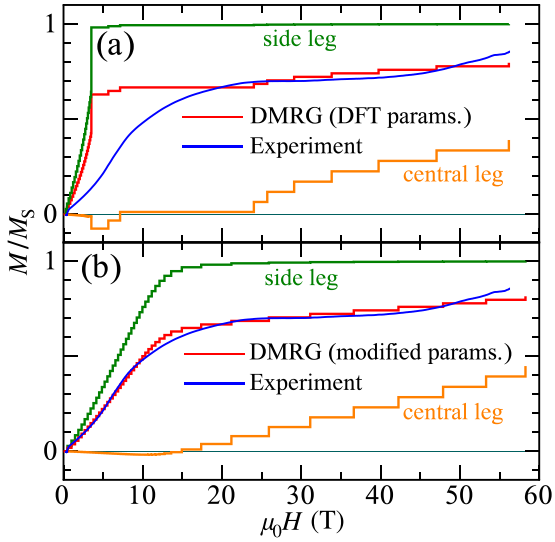

FIG. 2. Comparison of the magnetization curve measured on $Cu_3SO_4(OH)_4$ powder at 1.4 K (blue) against the DMRG simulation of the spin model (red). (a) Exchanges from Table I based on our refined crystal structure result in abrupt polarization of the side legs. (b) A modified parameter set (see text) improves the agreement. A g factor of 2.18 taken from ESR [27] was used for scaling B.

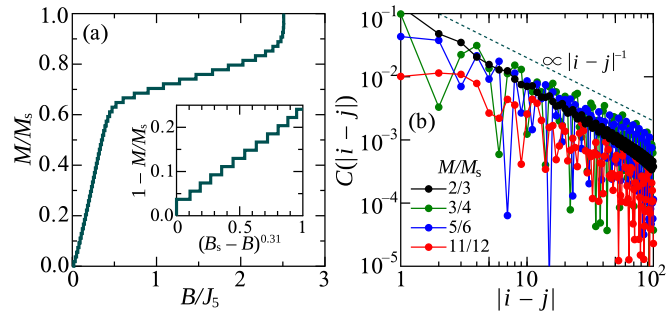

FIG. 3. (a) Full magnetization curve calculated by DMRG with the modified parameter set. Inset: Singular behavior of $1 - M/M_s$ vs $(B - B_s)^\gamma$ with $\gamma = 0.31$ near the saturation field. (b) Log-log plot of the spin-spin correlation function $C(|i - j|)$ as a function of distance along the central leg for several M/M_s values. The asymptotic behavior of the pure 1D AFM Heisenberg model, $\propto |i - j|^{-1}$, is shown as a guide.

Such a small energy difference suggests an exquisite sensitivity to the ratios of the exchange interactions, which would imply that the competition between collinear and helical states can be manipulated by perturbations such as chemical substitution, pressure, or magnetic field.

To determine the ground state of the quantum model, we performed density-matrix renormalization group (DMRG) simulations [36,37] using an open cluster of 40×3 spins; further details are in the Supplemental Material online [27]. The resulting spin correlations indicate a noncollinear state in which central as well as side legs are twisted into a helix. Similar to the classical model, other states have comparable energies. For instance, the enhancement of $|J_1|$ and $|J_2|$ and the reduction of J_6' readily stabilize the correct ground state [38]. More details on the energy balance of the competing phases are provided in the Supplemental Material [27].

To gain further confidence in the exchange parameters, we computed the longitudinal magnetization $\langle S^z \rangle$ by DMRG on a 36×3 cluster where periodic boundary conditions were applied along the ladder, and compared it with the experimental magnetization curve. While the field dependence of the magnetization for the parameter set from Table I is too steep [Fig. 2(a)], an effective description based on a modified set of parameters ($J_1 = -25.2$, $J_2 = -16.8$, $J_3 = 14.7$, $J_4 = 6.3$, $J_5 = 42.0$, $J_6 = 10.5$, $J_6' = 1.7$, and $J_7 = 6.7$ K; also see the Supplemental Material [27]) yields excellent agreement [Fig. 2(b)]. With the data at hand, we conclude that antlerite embodies a delicate balance of frustrated interactions operating within the central and side legs as well as connecting them into a ladder. Furthermore, by applying small perturbations, the appearance of fascinating phenomena caused by competition/collaboration between the Haldane physics and order-by-disorder mechanism is highly likely.

Finally, we comment on the magnetic state above the plateaulike feature at $M/M_s = 2/3$ for saturation magnetization M_s, which is not a plateau so much as a gradual upturn. This means that quantum fluctuations are strong, and the central leg is no longer fully AFM ordered, likely due to a loss of stabilizing interactions with the now-polarized side legs, which would also act to screen it from the neighboring ladders. Since this would render the central leg as an essentially ideal 1D Heisenberg spin system and an exotic field-induced Tomonaga-Luttinger liquid (TLL), it is worth looking closely at the DMRG results in this regime.

We find that the central leg may be regarded as an ideal 1D Heisenberg spin system at $M/M_s \geqslant 2/3$, implying a field-induced TLL phase. To confirm the TLL nature of the central leg at $M/M_s \geqslant 2/3$, we investigated the shape of the full magnetization curve [plotted vs. B/J_5 in Fig. 3(a)] as well as the asymptotic behavior of the spin-spin correlation function. At $M/M_s \sim 2/3$, the side legs are completely polarized by the field while the spin state of the central leg remains nearly singlet. Upon increasing B, the magnetization of the central leg then exhibits an initially slow increase and ultimately a singularity $dM/dB = \infty$ at the saturation field $B_s/J_5 \sim 2.5$. This behavior is typical of a 1D AFM Heisenberg system in a critical regime. Using perturbation theory, the form of the magnetization curve as $M \to M_s$ is known to be $1 - M/M_s \propto (B - B_s)^\gamma$, with $\gamma > 0$ [39]. Our calculated magnetization curve indeed takes this form, with $\gamma = 0.31$, as shown in the inset of Fig. 3(a). This γ value deviates from that of the pure 1D AFM Heisenberg chain with only nearest-neighbor coupling ($\gamma = 0.5$) due to the existence of next-nearest-neighbor coupling J_6. The spin-spin correlation function $C(|i - j|) = \langle S_i^z S_j^z \rangle - \langle S_i^z \rangle \langle S_j^z \rangle$ calculated by DMRG with a 160×3 open cluster is plotted as a function of distance $|i - j|$ in Fig. 3(b) for several M/M_s ($\geqslant 2/3$) values. In every case, a power-law decay is clearly evident. Interestingly, the decay ratios seem to be relatively close to the $\propto |i - j|^{-1}$ of the pure 1D AFM Heisenberg chain despite J_6, confirming that the central leg is a field-induced TLL for $2/3 \leqslant M/M_s \leqslant 1$.

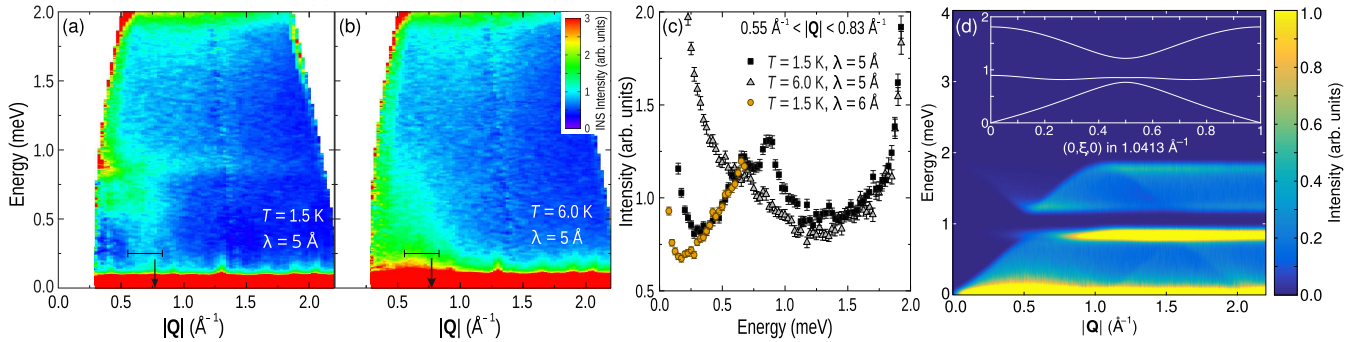

FIG. 4. Powder INS spectra of deuterated antlerite. Intensity maps at (a) 1.5 and (b) 6.0 K. (c) Temperature dependence of the intensity, averaged over the Q range identified by bars in (a) and (b); the 6-Å data were rescaled to match the 5-Å data at high energies. (d) Simulated spectra based on the modified DMRG parameters; main panel is powder averaged.

Powder INS spectra collected at 1.5 and 6.0 K to validate the model parameters are shown in Figs. 4(a) and 4(b) and to higher energy in the Supplemental Material online [27]. Peaks in the magnetic intensity at energies of ∼0.6 and 0.8 meV may correlate to the narrow band and the bottom of the upper magnon band in Fig. 4(d), calculated based on the DMRG exchange parameters above. This intensity vanishes for higher momentum transfer Q and higher temperatures [Fig. 4(c)] as expected for a magnetic signal, and appears to disperse to a minimum near the propagation vector (black arrows). The calculated exchange parameters can evidently describe the key features of the spectrum, aside from an overall scale factor that is likely associated with the uncertainties of DFT or quantum renormalization, supporting the ratios among our J parameters. Flat magnon bands have been predicted in sawtooth and kagome lattices [40], where they may be a potential platform for magnon crystals, nontrivial magnon topology, and non-Hermitian exceptional points [41], and it would be interesting if the narrow feature around 0.8 meV proved to be such a flat magnon band.

The low-temperature magnetic state we find in $Cu_3SO_4(OH)_4$ contains all the essential ingredients found in botallackite: a low-dimensional Cu^{2+} spin system with mutually antialigned FM legs, separated by an AFM leg with a spin orientation tilted by a significant angle relative to the FM spin orientation, linked through a distorted-triangular motif. This suggests that antlerite may also realize the spinon-magnon mixing recently proposed in botallackite [10] and thus far reported in no other materials. The key difference is that in botallackite these legs alternate in a two-dimensional sheet, whereas in antlerite they form quasi-one-dimensional three-leg ladders with very weak interladder coupling. In antlerite, we find that the magnetic ground state is on the cusp of several other potential ground states, which are closely spaced in energy, suggesting that the magnetic ground state may be readily tuned, for instance by applied field, strain, or chemical substitution. In fact, when we first calculated the magnetic ground state starting from the atomic positions reported in Ref. [16], we obtained a Haldane-like up-up-down-down magnetic ground state distinct from those discussed here. Since the reported structure differs from ours chiefly in interladder hydrogen positions irrelevant to the intrachain interactions, this is further evidence of an extreme sensitivity to perturbations. Besides idle-spin cycloidal order reported upon isoelectronic substitution of S by Se [42], which could perhaps be revisited in light of the non-idle-spin magnetism found here, a cascade of phase transitions have been reported with temperature and in applied magnetic fields [17,19,43], to which we now add the high-field plateau. We also note that szenicsite $Cu_3MoO_4(OH)_4$ has a similar three-leg ladder motif [44], but with a different alternation of exchange parameters which leads the outer chains to dimerize into a classical spin-1 system [45]. The synthesis of szenicite has not been reported, but substitution of S by Mo may offer not only a further route for tuning the magnetism, but feedback on how to grow this Mo analog.

The distorted triangular lattice motifs found in Cu-based minerals have already revealed a number of interesting exotic magnetic phases, and antlerite stands to serve as an excellent platform for exploring their wealth of physics. The interchain exchanges in $Cu_3SO_4(OH)_4$ give rise to a model with a rich phase diagram that should be readily explored experimentally thanks to the advantageous energy scales.

We thank Ulrike Nitzsche for technical assistance. This project was funded by the German Research Foundation (DFG) via the projects A05, C01, C03, and C06 of the Collaborative Research Center SFB 1143 (project-id 247310070); GRK 1621 (project-id 129760637); the Würzburg-Dresden Cluster of Excellence on Complexity and Topology in Quantum Matter—*ct.qmat* (EXC 2147, project-id 390858490); through individual research grants, Grants No. IN 209/9-1 and No. PE 3318/2-1; and through project-id 422219907. D.K. and O.J. were supported by the Leibniz Association through the Leibniz Competition. The authors acknowledge the Institut Laue-Langevin, Grenoble (France) for providing neutron beam time [46,47], and the HLD at HZDR, member of the European Magnetic Field Laboratory (EMFL). Part of this work is based on experiments performed at the Swiss spallation neutron source SINQ, Paul Scherrer Institute, Villigen, Switzerland.

[1] O. A. Starykh, Unusual ordered phases of highly frustrated magnets: A review, Rep. Prog. Phys. **78**, 052502 (2015).

[2] H. T. Diep, *Frustrated Spin Systems*, 2nd ed. (World Scientific, Singapore, 2013).

[3] T. A. Kaplan and N. Menyuk, Spin ordering in three-dimensional crystals with strong competing exchange interactions, Philos. Mag. **87**, 3711 (2007).

[4] *Introduction to Frustrated Magnetism*, edited by C. Lacroix, P. Mendels, and F. Mila, Springer Series in Solid-State Sciences Vol. 164 (Springer, Berlin, 2011).

[5] A. P. Ramirez, Strongly geometrically frustrated magnets, Annu. Rev. Mater. Sci. **24**, 453 (1994).

[6] C. D. Batista, S.-Z. Lin, S. Hayami, and Y. Kamiya, Frustration and chiral orderings in correlated electron systems, Rep. Prog. Phys. **79**, 084504 (2016).

[7] B. Schmidt and P. Thalmeier, Frustrated two dimensional quantum magnets, Phys. Rep. **703**, 1 (2017).

[8] D. S. Inosov, Quantum magnetism in minerals, Adv. Phys. **67**, 149 (2018).

[9] L. Testa, V. Šurija, K. Prša, P. Steffens, M. Boehm, P. Bourges, H. Berger, B. Normand, H. M. Rønnow, and I. Živković, Triplons, magnons, and spinons in a single quantum spin system: $SeCuO_3$, Phys. Rev. B **103**, L020409 (2021).

[10] H. Zhang, Z. Zhao, D. Gautreau, M. Raczkowski, A. Saha, V. O. Garlea, H. Cao, T. Hong, H. O. Jeschke, S. D. Mahanti, T. Birol, F. F. Assaad, and X. Ke, Coexistence and Interaction of Spinons and Magnons in an Antiferromagnet with Alternating Antiferromagnetic and Ferromagnetic Quantum Spin Chains, Phys. Rev. Lett. **125**, 037204 (2020).

[11] F. C. Hawthorne, Refinement of the crystal structure of botallackite, Mineral. Mag. **49**, 87 (1985).

[12] D. M. Gautreau, A. Saha, and T. Birol, First-principles characterization of the magnetic properties of $Cu_2(OH)_3Br$, Phys. Rev. Materials **5**, 024407 (2021).

[13] K. Majumdar and S. D. Mahanti, Quantum fluctuation effects on the ordered moments in a two dimensional frustrated ferrimagnet, J. Phys.: Condens. Matter **33**, 125801 (2021).

[14] F. C. Hawthorne, L. A. Groat, and R. R. Eby, Antlerite, $Cu_3SO_4(OH)_4$, a heteropolyhedral wallpaper structure, Can. Mineral. **27**, 205 (1989).

[15] S. van Smaalen, Structural aspects of spin-chain and spin-ladder oxides, Z. Krist. - Cryst. Mater. **214**, 786 (1999).

[16] S. Vilminot, M. Richard-Plouet, G. André, D. Swierczynski, M. Guillot, F. Bourée-Vigneron, and M. Drillon, Magnetic structure and properties of $Cu_3(OH)_4SO_4$ made of triple chains of spins $s = 1/2$, J. Solid State Chem. **170**, 255 (2003).

[17] S. Hara, H. Kondo, and H. Sato, Successive magnetic transitions in candidate "idle-spin" system, $Cu_3(OH)_4SO_4$, J. Phys. Soc. Jpn. **80**, 043701 (2011).

[18] H.-J. Koo, R. K. Kremer, and M.-H. Whangbo, Non-idle-spin behavior and field-induced magnetic transitions of the triple chain magnet $Cu_3(OH)_4SO_4$, J. Phys. Soc. Jpn. **81**, 063704 (2012).

[19] Y. Fujii, Y. Ishikawa, H. Kikuchi, Y. Narumi, H. Nojiri, S. Hara, and H. Sato, Magnetic property of a single crystal of spin-1/2 triple-chain magnet $Cu_3(OH)_4SO_4$, J. Korean Phys. Soc. **62**, 2054 (2013).

[20] G. M. Sheldrick, A short history of SHELX, Acta Crystallogr., Sect. A: Found. Adv. **64**, 112 (2008).

[21] G. M. Sheldrick, Crystal structure refinement with SHELXL, Acta Crystallogr. Sect. C: Struct. Chem. **71**, 3 (2015).

[22] L. J. Farrugia, WINGX and ORTEP for WINDOWS: An update, J. Appl. Crystallogr. **45**, 849 (2012).

[23] I. Puente Orench, J. F. Clergeau, S. Martínez, M. Olmos, O. Fabelo, and J. Campo, The new powder diffractometer D1B of the Institut Laue Langevin, J. Phys.: Conf. Ser. **549**, 012003 (2014).

[24] T. Fennell, L. Mangin-Thro, H. Mutka, G. J. Nilsen, and A. R. Wildes, Wavevector and energy resolution of the polarized diffuse scattering spectrometer D7, Nucl. Instrum. Methods Phys. Res., Sect. A **857**, 24 (2017).

[25] J. Rodríguez-Carvajal, Recent advances in magnetic structure determination by neutron powder diffraction, Phys. B: Condens. Matter **192**, 55 (1993).

[26] V. F. Sears, Neutron scattering lengths and cross sections, Neutron News **3**, 26 (1992).

[27] See Supplemental Material at http://link.aps.org/supplemental/10.1103/PhysRevB.106.L020405 for further experimental details, additional results of the structure and magnetic refinements, crystallographic information files describing our refinements, and for additional information on the band-structure calculation and the model simulations, which includes Refs. [48–56].

[28] S. Janßen, J. Mesot, L. Holitzner, A. Furrer, and R. Hempelmann, FOCUS: A hybrid TOF-spectrometer at SINQ, Phys. B (Amsterdam, Neth.) **234-236**, 1174 (1997).

[29] S. Toth and B. Lake, Linear spin wave theory for single-Q incommensurate magnetic structures, J. Phys.: Condens. Matter **27**, 166002 (2015).

[30] Y. Skourski, M. D. Kuz'min, K. P. Skokov, A. V. Andreev, and J. Wosnitza, High-field magnetization of Ho_2Fe_{17}, Phys. Rev. B **83**, 214420 (2011).

[31] S. Vilminot, M. Richard-Plouet, G. André, D. Swierczynski, F. Bourée-Vigneron, E. Marino, and M. Guillot, Synthesis, structure and magnetic properties of copper hydroxysulfates, Cryst. Eng. **5**, 177 (2002).

[32] S. Okubo, H. Yamamoto, M. Fujisawa, H. Ohta, T. Nakamura, and H. Kikuchi, High field ESR measurements of quantum triple chain system $Cu_3(OH)_4SO_4$, J. Phys.: Conf. Ser. **150**, 042156 (2009).

[33] K. Koepernik and H. Eschrig, Full-potential nonorthogonal local-orbital minimum-basis band-structure scheme, Phys. Rev. B **59**, 1743 (1999).

[34] J. P. Perdew, K. Burke, and M. Ernzerhof, Generalized Gradient Approximation Made Simple, Phys. Rev. Lett. **77**, 3865 (1996).

[35] Interladder exchange interactions are on the order of fractions of a kelvin, two orders of magnitude weaker than the dominant intraladder exchanges. While they play a key role in producing three-dimensional long-range order, they have negligible impact on the type of order or the physics within a ladder.

[36] S. R. White, Density Matrix Formulation for Quantum Renormalization Groups, Phys. Rev. Lett. **69**, 2863 (1992).

[37] S. R. White, Density-matrix algorithms for quantum renormalization groups, Phys. Rev. B **48**, 10345 (1993).

[38] The small mutual noncollinearity of side legs stems from the exchange anisotropy and cannot be accounted for in the (isotropic) Heisenberg model.

[39] J. B. Parkinson and J. C. Bonner, Spin chains in a field:

Crossover from quantum to classical behavior, Phys. Rev. B **32**, 4703 (1985).

[40] O. Derzhko, J. Richter, and M. Maksymenko, Strongly correlated flat-band systems: The route from Heisenberg spins to Hubbard electrons, Int. J. Mod. Phys. B **29**, 1530007 (2015).

[41] P. A. McClarty, M. Haque, A. Sen, and J. Richter, Disorder-free localization and many-body quantum scars from magnetic frustration, Phys. Rev. B **102**, 224303 (2020).

[42] S. Vilminot, G. André, F. Bourée-Vigneron, M. Richard-Plouet, and M. Kurmoo, Magnetic properties and magnetic structures of $Cu_3(OD)_4XO_4$, X = Se or S: Cycloidal versus collinear antiferromagnetic structure, Inorg. Chem. **46**, 10079 (2007).

[43] A. A. Kulbakov, E. Sadrollahi, F. Rasch, M. Avdeev, S. Gaß, L. T. Corredor Bohorquez, A. U. B. Wolter, M. Feig, R. Gumeniuk, H. Poddig, M. Stötzer, F. J. Litterst, I. Puente-Orench, A. Wildes, E. Weschke, J. Geck, D. S. Inosov, and D. C. Peets, Incommensurate and multiple-q magnetic misfit order in the frustrated quantum spin ladder material antlerite, $Cu_3SO_4(OH)_4$, arXiv:2207.05606 [cond-mat.str-el].

[44] M. Fujisawa, H. Kikuchi, Y. Fujii, S. Mitsudo, A. Matsuo, and K. Kindo, New category of the frustrated quantum magnets composed of spin-1/2 triple-chains, J. Phys.: Conf. Ser. **320**, 012031 (2011).

[45] S. Lebernegg, O. Janson, I. Rousochatzakis, S. Nishimoto, H. Rosner, and A. A. Tsirlin, Frustrated spin chain physics near the Majumdar-Ghosh point in szenicsite $Cu_3(MoO_4)(OH)_4$, Phys. Rev. B **95**, 035145 (2017).

[46] D. S. Inosov, A. A. Kulbakov, D. C. Peets, and I. Puente-Orench, Determining the zero-field magnetic structure of antlerite, Institut Laue-Langevin (ILL), Grenoble, doi:10.5291/ILL-DATA.5-31-2734.

[47] D. S. Inosov, A. A. Kulbakov, A. Mannathanath Chakkingal, D. C. Peets, and A. Wildes, Verifying the magnetic origin of the low-temperature diffuse signal in antlerite powder, Institut Laue-Langevin (ILL), Grenoble, doi:10.5291/ILL-DATA.5-32-923.

[48] Bruker, APEX3 v2018.1-0, Bruker AXS Inc., Madison, WI.

[49] S. A. Zvyagin, J. Krzystek, P. H. M. van Loosdrecht, G. Dhalenne, and A. Revcolevschi, High-field ESR study of the dimerized-incommensurate phase transition in the spin-Peierls compound $CuGeO_3$, Phys. B (Amsterdam, Neth.) **346-347**, 1 (2004).

[50] A. S. Wills, A new protocol for the determination of magnetic structures using simulated annealing and representational analysis (SARA*h*), Phys. B (Amsterdam, Neth.) **276-278**, 680 (2000).

[51] M. Oshikawa and I. Affleck, Electron spin resonance in $S = \frac{1}{2}$ antiferromagnetic chains, Phys. Rev. B **65**, 134410 (2002).

[52] V. I. Anisimov, J. Zaanen, and O. K. Andersen, Band theory and Mott insulators: Hubbard U instead of Stoner I, Phys. Rev. B **44**, 943 (1991).

[53] H. Eschrig and K. Koepernik, Tight-binding models for the iron-based superconductors, Phys. Rev. B **80**, 104503 (2009).

[54] C. E. Agrapidis, S.-L. Drechsler, J. van den Brink, and S. Nishimoto, Crossover from an incommensurate singlet spiral state with a vanishingly small spin gap to a valence-bond solid state in dimerized frustrated ferromagnetic spin chains, Phys. Rev. B **95**, 220404(R) (2017).

[55] S. Nishimoto, S.-L. Drechsler, R. O. Kuzian, J. van den Brink, J. Richter, W. E. A. Lorenz, Y. Skourski, R. Klingeler, and B. Büchner, Saturation Field of Frustrated Chain Cuprates: Broad Regions of Predominant Interchain Coupling, Phys. Rev. Lett. **107**, 097201 (2011).

[56] S. Qin, S. Liang, Z. Su, and L. Yu, Density-matrix renormalization-group calculation of correlation functions in the one-dimensional Hubbard model, Phys. Rev. B **52**, R5475 (1995).